Comparing quantumness criteria

Jérôme Martin, Amaury Micheli, Vincent Vennin

Comparing quantumness criteria

Jérôme Martin[1], Amaury Micheli,[2,1] and Vincent Vennin[3,1]

[1] *Institut d'Astrophysique de Paris, CNRS & Sorbonne Université, UMR 7095 98 bis boulevard Arago, 75014 Paris, France*
[2] *Université Paris-Saclay, CNRS/IN2P3, IJCLab, 91405, Orsay, France*
[3] *Laboratoire de Physique de l'Ecole Normale Supérieure, ENS, CNRS, Université PSL, Sorbonne Université, Université Paris Cité, F-75005 Paris, France*

Abstract –Measuring the quantumness of a system can be done with a variety of methods. In this article we compare different criteria, namely quantum discord, Bell inequality violation and non-separability, for systems placed in a Gaussian state. When the state is pure, these criteria are equivalent, while we find that they do not necessarily coincide when decoherence takes place. Finally, we prove that these criteria are essentially controlled by the semi-minor axis of the ellipse representing the state's Wigner function in phase space.

Introduction. – The characterisation of "classicality" and "quantumness" in quantum systems has become a topic of major importance in several branches of modern physics. Indeed, maybe surprisingly, it is not always trivial to establish whether a system behaves "classically" or "quantum-mechanically". This question is especially important when one tries to understand the nature of a physical phenomenon.

For instance, in cosmology, it is well-known that primordial perturbations are very well reproduced [20] by vacuum quantum fluctuations, amplified by gravitational instability [8, 33, 35, 60, 61, 75] during an early epoch of accelerated expansion named inflation [5, 32, 46, 47, 69, 74]. However, the quantum origin of those primordial perturbations has never been tested directly and, in practice, they are mostly treated by astronomers as classical, stochastic fluctuations. The reason why this is possible is that, under peculiar circumstances, and for certain observables, a quantum system can be mimicked by a classical one [45, 51, 53]. However, if a genuine quantum signature could be detected in cosmological observables, that would shed light on fundamental issues such as the need to quantise gravitational degrees of freedom or the emergence of classicality at cosmological scales [7, 49, 55, 59, 64, 78].

The same need to distinguish classical from quantum processes appears in analogue gravity, where phenomena involving gravitational physics are mapped to condensed-matter systems. In these setups, particles can either be created by quantum channels or by the classical amplification of a thermal bath [12]. The latter mechanism is always present when conducting

experiments at finite temperature. A quantum test is a way to tell the two populations apart and to demonstrate the existence of a quantum channel in these experiments [12, 40, 68, 76].

In quantum technologies, the distinction between quantum and classical behaviours is also central, since "quantumness" is a crucial resource e.g. in quantum computing [43] and quantum cryptography [21, 66].

This has led various notions of "quantumness" to be put forward. One possible approach is to consider correlations between sub-parts of a given system, and to determine whether or not they can be reproduced by classical random variables. This route gave rise to the celebrated Bell inequalities [6, 18, 29], quantum steering [83], different measures of entanglement (non-separability [81], multipartite entanglement [38], entanglement witnesses [37], *etc.*), quantum discord [11, 36, 63], *etc.*.

Another possible approach, leading to a second class of criteria, is to make use of phase-space formulations of quantum mechanics. For instance, the non-positivity of the Wigner function [82] or the absence of the P-representation [28, 77] have been viewed as criteria signalling the quantumness of a system [26, 80].

How these different criteria are related is a non-trivial question. In pure states, it is known that quantum discord reduces to entanglement entropy [11], which only vanishes in separable states, and that all non-separable states violate a Bell inequality [81]. For mixed states however, these relations become more elusive (for instance non-separability is only a necessary condition for Bell-inequality violation [81]).

In this article, our goal is to investigate the relations between different criteria in a subclass of quantum states where explicit calculations can be performed. We want to determine in which cases they lead to the same conclusion regarding the quantumness of a system, and in which cases they differ. In practice, we consider two continuous degrees of freedom placed in two-mode squeezed thermal states and analyse the link between three quantum criteria: non-separability, quantum discord and a Bell inequality.

Gaussian states. – Let us consider two continuous degrees of freedom q_1 and q_2, with conjugated momenta p_1 and p_2, arranged into the phase-space vector $\hat{\boldsymbol{R}}_{1/2} = (\hat{q}_1, \hat{p}_1, \hat{q}_2, \hat{p}_2)^{\mathrm{T}}$ with $[\hat{q}_i, \hat{p}_j] = i\delta_{ij}$. Their quantum state is represented by the density matrix $\hat{\rho}$. For a given quantum operator $\hat{O}$, the Weyl transform

$$\tilde{O}(\boldsymbol{R}_{1/2}) \equiv \int \mathrm{d}u_1\, \mathrm{d}u_2\, e^{-ip_1u_1 - ip_2u_2} \times \left\langle q_1 + \frac{u_1}{2}, q_2 + \frac{u_2}{2} \middle| \hat{O} \middle| q_1 - \frac{u_1}{2}, q_2 - \frac{u_2}{2} \right\rangle \quad (1)$$

yields a scalar function in phase space. The Wigner function W is the Weyl transform of the density matrix [16], $W = \tilde{\rho}/(2\pi)^2$, and is such that the expectation value of any quantum operator $\hat{A}$ is given by the phase-space average of its Weyl transform against the Wigner function,

$$\left\langle \hat{A} \right\rangle = \int \tilde{A}\left(\boldsymbol{R}_{1/2}\right) W(\boldsymbol{R}_{1/2})\, \mathrm{d}^4\boldsymbol{R}_{1/2}\,. \quad (2)$$

This is why the Wigner function is often referred to as a "quasi-probability" distribution function.

A Gaussian state is defined as a state whose Wigner function is Gaussian. All information about the state is then contained in the covariance matrix

$$\gamma_{ab} = \langle \{\hat{R}_a, \hat{R}_b\} \rangle\,, \quad (3)$$

where $\hat{R}_a$ refers to the components of the vector $\hat{\boldsymbol{R}}_{1/2}$, $\{\hat{A}, \hat{B}\} = \hat{A}\hat{B} + \hat{B}\hat{A}$ is the anti-commutator and the Wigner function reads

$$W(\boldsymbol{R}_{1/2}) = \frac{1}{\pi^2\sqrt{\det\boldsymbol{\gamma}}} \exp\left(-\boldsymbol{R}_{1/2}^{\mathrm{T}}\boldsymbol{\gamma}^{-1}\boldsymbol{R}_{1/2}\right)\,. \quad (4)$$

Let us also introduce the purity $p \equiv \mathrm{Tr}(\hat{\rho}^2)$, which determines whether the state is pure ($p = 1$) or mixed ($p < 1$). For a Gaussian state, the purity is directly related to the determinant of the covariance matrix [2]

$$p = \frac{1}{\sqrt{\det\boldsymbol{\gamma}}}\,. \quad (5)$$

Two-mode squeezed vacuua (TMSV) are Gaussian states whose covariance matrix depend on two parameters only, r and φ, respectively called squeezing amplitude and squeezing angle, and reads [9, 17, 70]

$$\boldsymbol{\gamma}^{\mathrm{TMSV}} \equiv \begin{pmatrix} \boldsymbol{\gamma}^{11} & \boldsymbol{\gamma}^{12} \\ \boldsymbol{\gamma}^{21} & \boldsymbol{\gamma}^{22} \end{pmatrix}, \tag{6}$$

with

$$\boldsymbol{\gamma}^{11} = \boldsymbol{\gamma}^{22} \equiv \cosh(2r)\mathbb{1}_2, \tag{7}$$

and

$$\boldsymbol{\gamma}^{12} = \boldsymbol{\gamma}^{21} \equiv -\sinh 2r \begin{pmatrix} \cos 2\varphi & \sin 2\varphi \\ \sin 2\varphi & -\cos 2\varphi \end{pmatrix}. \tag{8}$$

TMSV are ubiquitous in modern physics : they appear in quantum optics [9, 17, 70], cold atoms [22, 62] as well as in the study of inflation [3, 19, 30, 31] and Hawking radiation [4, 34]. Using Eq. (5) one can check that they are pure. In general, TMSV may become mixed as an effect of decoherence [42, 84, 85]. We will consider the class of two-mode squeezed thermal states which are defined as Gaussian states with covariance matrices of the form

$$\boldsymbol{\gamma} = \frac{\boldsymbol{\gamma}^{\mathrm{TMSV}}}{\sqrt{p}}, \tag{9}$$

where one can check from Eq. (5) that p is indeed the purity of the state. These states arise for instance for cosmological perturbations linearly coupled to an environment while preserving statistical homogeneity [15, 50], or when an initial TMSV interacts with two identical independent thermal baths [23, 48], or when the modes are sent through a pure-loss or an additive Gaussian noise channel [25]. The two latter channels are described by simple transformations of the covariance matrix, respectively given by $\boldsymbol{\gamma} = \eta\boldsymbol{\gamma}^{\mathrm{TMSV}} + (1-\eta)\,\mathbb{1}_4$ where the efficiency parameter $0 \leq \eta \leq 1$ encodes the level of loss/damping experienced across the channel, and $\boldsymbol{\gamma} = \boldsymbol{\gamma}^{\mathrm{TMSV}} + \Delta\mathbb{1}_4$ where $\Delta \geq 0$ encodes the level of noise. Both matrices can then be put in the form (9), with effective squeezing and purity parameters given in Eqs. (66) and (70) of the Appendix where these two channels are studied in details.

In the following we work in terms of these effective squeezing and purity parameters, such that all setups mentioned above are encompassed in the analysis. Decoherence is expected to play a key role in the emergence of classicality, and this simply parameterised class of states will allow us to study how different criteria respond to it.

Under a canonical transformation, $\hat{\boldsymbol{R}} \to \boldsymbol{T}\hat{\boldsymbol{R}}$, where $\boldsymbol{T}$ is a symplectic matrix (i.e. it preserves commutation relations), the covariance matrix changes according to $\boldsymbol{\gamma} \to \boldsymbol{T}\boldsymbol{\gamma}\boldsymbol{T}^{\mathrm{T}}$. This implies that the covariance matrix depends on the set of canonical variables used to describe a system.

For instance, there exists a partition $\hat{\boldsymbol{R}}_{\mathrm{D}}$ where the covariance matrix is block diagonal,

$$\gamma^{\mathrm{D}} = \frac{1}{\sqrt{p}} \begin{pmatrix} \gamma^{\mathrm{OMSV}} & 0 \\ 0 & \gamma^{\mathrm{OMSV}} \end{pmatrix}, \tag{10}$$

with

$$\gamma^{\mathrm{OMSV}} \equiv \begin{pmatrix} \gamma_{qq} & \gamma_{qp} \\ \gamma_{pq} & \gamma_{pp} \end{pmatrix} \tag{11}$$

and

$$\gamma_{qq} = [\cosh(2r) - \cos(2\varphi)\sinh(2r)], \tag{12}$$
$$\gamma_{pq} = \gamma_{\mathrm{qp}} = -\sin(2\varphi)\sinh(2r), \tag{13}$$
$$\gamma_{pp} = [\cosh(2r) + \cos(2\varphi)\sinh(2r)], \tag{14}$$

such that the Wigner function factorises according to $W^{\mathrm{D}}(\boldsymbol{R}^{\mathrm{D}}) = \bar{W}(q_1^{\mathrm{D}}, p_1^{\mathrm{D}})\bar{W}(q_2^{\mathrm{D}}, p_2^{\mathrm{D}})$. In this basis, the quantum state is nothing but the product of two identical and uncorrelated one-mode squeezed (thermal) states. If $p = 1$ they are one-mode squeezed vacuua (OMSV).

This also implies that quantumness criteria, which characterise the correlations between two subsystems, obviously depend on the way the system is partitioned (for instance, the way quantum discord depends on the choice of partition has been studied in Refs. [50, 52]).

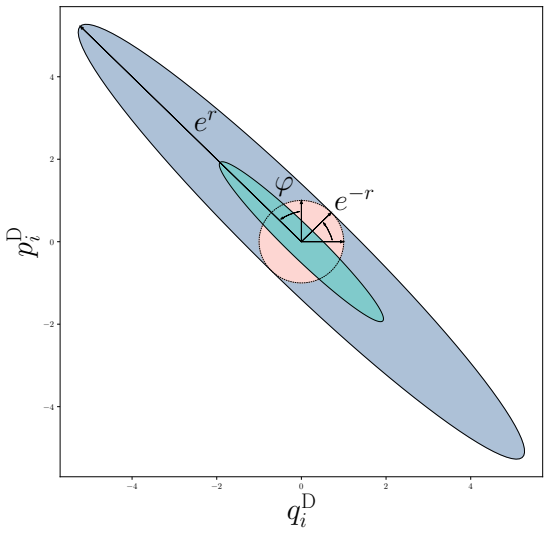

Fig. 1: Phase-space $\sqrt{2}$-σ contour levels of the Wigner function $\bar{W}$. The pink circle corresponds to a vacuum state (coherent state) with $p = 1$ and vanishing squeezing parameter $r = 0$. The green ellipse represents a pure state $p = 1$, slightly squeezed $r = 1$ along the diagonal $\varphi = \pi/4$. The blue ellipse represents a state with the same squeezing parameter $r = 1$ but with purity $p = e^{-4} \approx 0.018$ such that its semi-minor axis is of the same size as in the vacuum state.

In practice, their often exists a "preferred" basis of operators corresponding to separately measurable physical degrees of freedom [56, 57] The factorised partition (10) is nonetheless useful as it provides a simple geometric representation of the quantum state: the contours of $\bar{W}$ are ellipses in the phase space $(q_i^{\mathrm{D}}, p_i^{\mathrm{D}})$, as displayed in Fig. 1. Their eccentricity is controlled by r, φ is the angle between the q_i^{D}-axis and the semi-minor axis, and the area contained in the ellipses is proportional to $1/p$.

Quantumness criteria. – Since the quantum states we consider are fully characterised by the three parameters r, φ and p, let us express the three quantumness criteria in terms of these parameters, in order to compare them.

Quantum Discord. A first way to characterise the presence of quantum correlations between two sub-parts of a system is by quantum discord [36, 63]. The idea is to introduce two measures of correlation that coincide for classically correlated setups thanks to Bayes' theorem, but that may differ for quantum systems. The first measure is the so-called mutual information $\mathcal{I}$, which is the sum between the von-Neumann entropy of both reduced sub-systems, minus the entropy of the entire system. The second measure $\mathcal{J}$ evaluates the difference between the entropy contained in the first subsystem, and the entropy contained in that same subsystem when the second subsystem has been measured, where an extremisation is performed over all possible ways to "measure" the second subsystem. $\mathcal{J}$ can be shown to be always less than $\mathcal{I}$. Quantum discord $\mathcal{D}$ is defined as the difference between these two measures and is thus a positive quantity that only vanishes for classical systems.

For Gaussian states, $\mathcal{I}$, $\mathcal{J}$ and $\mathcal{D}$ can be expressed in terms of the local symplectic invariants of the covariance matrix [2].[1] It is shown in [1, 27, 65] that, for covariance matrices of the form (9), quantum discord depends on r and p only and is given by

$$\begin{aligned}\mathcal{D}(p,r) =& f\left[\sigma(p,r)\right] - 2f\left(p^{-1/2}\right) \\ &+ f\left[\frac{\sigma(p,r)+p^{-1}}{\sigma(p,r)+1}\right], \end{aligned} \tag{15}$$

where the function $f(x)$ is defined for $x \geq 1$ by

$$\begin{aligned} f(x) \equiv& \left(\frac{x+1}{2}\right)\log_2\left(\frac{x+1}{2}\right) \\ &- \left(\frac{x-1}{2}\right)\log_2\left(\frac{x-1}{2}\right), \end{aligned} \tag{16}$$

[1] This means that quantum discord is invariant under local symplectic transformations, i.e. those mixing q_i with p_i but not with q_j and p_j. This explains why φ does not appear in the final expression (15), since it can be changed arbitrarily by performing phase-space rotations in each sector.

and

$$\sigma(p,r) = \frac{\cosh(2r)}{\sqrt{p}}\,. \tag{17}$$

Note that in the partition (10), where the covariance matrix is block-diagonal, the two subsystems are uncorrelated hence quantum discord vanishes.

Bell Inequality. Another way to characterise the presence of quantum correlations is via Bell inequalities [10]. When violated, they allow one to exclude classical and realistic local theories [58]. Usually designed for discrete observables [18](such as spins), they can also be applied to continuous variables by means of pseudo-spin operators [6, 29] or via projections on coherent states [14]. In this paper we will use the pseudo-spin operators introduced in Ref. [29]

$$\hat{\sigma}_x^i = \int_{-\infty}^{\infty} \mathrm{sign}(q_i)\,|q_i\rangle\langle q_i|\,\mathrm{d}q_i\,, \tag{18}$$

$$\hat{\sigma}_y^i = -i\int_{-\infty}^{\infty} \mathrm{sign}(q_i)\,|q_i\rangle\langle -q_i|\,\mathrm{d}q_i\,, \tag{19}$$

$$\hat{\sigma}_z^i = -\int_{-\infty}^{\infty} |q_i\rangle\langle -q_i|\,\mathrm{d}q_i\,. \tag{20}$$

One can check that these operators satisfy the SU(2) commutation relations

$$\left[\hat{\sigma}_\mu^i, \hat{\sigma}_\nu^j\right] = 2i\epsilon_{\mu\nu\lambda}\hat{\sigma}_\lambda^i\delta^{ij}\,, \tag{21}$$

where $\epsilon_{\mu\nu\lambda}$ is the totally anti-symmetric tensor.

From these operators we can build a Bell inequality [29, 54]

$$\langle\hat{B}\rangle = 2\sqrt{\langle\hat{\sigma}_z^1\hat{\sigma}_z^2\rangle^2 + \langle\hat{\sigma}_x^1\hat{\sigma}_x^2\rangle^2} \leq 2. \tag{22}$$

In order to compute the two-point correlation functions of the operators $\hat{\sigma}_x$ and $\hat{\sigma}_z$, one can derive their Weyl transform and make use of Eq. (2). Since $\hat{\sigma}_\mu^1$ and $\hat{\sigma}_\mu^2$ act on different degrees of freedom, the Weyl transform of their product factorises as

$$\widetilde{\sigma_\mu^1\sigma_\nu^2} = \widetilde{\sigma_\mu^1}\widetilde{\sigma_\nu^2}\,, \tag{23}$$

and in the appendix we show that

$$\widetilde{\sigma_z^i} = -\pi\delta(q_i)\delta(p_i), \quad \widetilde{\sigma_x^i} = \mathrm{sgn}(q_i)\,, \tag{24}$$

where δ stands for the Dirac distribution. Together with Eq. (2), this leads to

$$\left\langle\hat{\sigma}_z^i\hat{\sigma}_z^j\right\rangle = p\,, \tag{25}$$

$$\left\langle\hat{\sigma}_x^i\hat{\sigma}_x^j\right\rangle = -\frac{2}{\pi}\arcsin\left[|\cos(2\varphi)|\tanh(2r)\right]\,. \tag{26}$$

Inserting Eqs. (25) and (26) into Eq. (22) leads to

$$\langle\hat{B}\rangle = 2\sqrt{p^2 + \frac{4}{\pi^2}\arcsin^2\left[\cos(2\varphi)\tanh(2r)\right]}\,. \tag{27}$$

Compared to quantum discord given in Eq. (15), one can see that the mean value of the Bell operator $\langle\hat{B}\rangle$ depends on the squeezing angle φ in addition to the squeezing amplitude r and the purity p. This is expected since the operators given in Eq. (18) are not invariant under local symplectic transformations.

Non-separability. Finally we consider quantum separability. A state is said to be separable in a certain partition if its density matrix can be written as a statistical mixture of products of density matrices over the two sub-systems, i.e.

$$\hat{\rho} = \sum_i \alpha_i\hat{\rho}_1^i \bigotimes \hat{\rho}_2^i, \tag{28}$$

where α_i are real coefficients. In general, proving that a state is separable is a non-trivial task, yet, for Gaussian states, the so-called Peres-Horodecki criterion was proven to be necessary and sufficient [72]. In the appendix we show how to evaluate this criterion for Gaussian states, in a one-parameter family of partitions that contains both Eq. (9) and Eq. (10). In the partition corresponding to Eq. (10), the state is, as expected, always separable, while for Eq. (9) we find that the state is separable if and only if

$$e^{-2r} \geq \sqrt{p}\,. \tag{29}$$

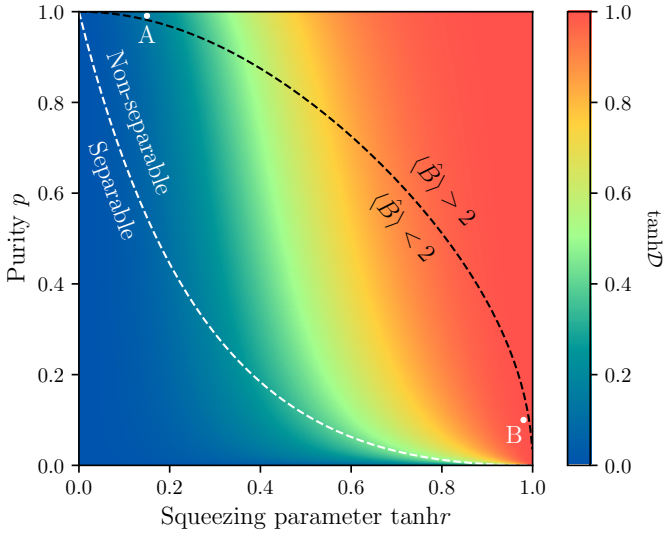

Fig. 2: Hyperbolic tangent of the quantum discord $\tanh\mathcal{D}$ computed from Eq. (15) as a function of the purity p and the hyperbolic tangent of the squeezing parameter $\tanh r$. The dashed white (respectively black) line represents the threshold of separability (respectively Bell inequality violation) defined as the equality case in Eq. (29) [respectively Eq. (27)].

Results & Discussion. – Let us first make connection with the phase-space approaches mentioned in the introduction. We point out that the thermal squeezed states considered here always have a *positive* Wigner phase-space probability distribution, which could make them appear classical. Yet, as demonstrated, these states can exhibit quantum features. We refer to Refs. [24, 49, 67] for detailed discussions of this point. Additionally, for these states, the absence of a Glauber-Sudarshan P-representation, which is considered as a sign of non-classicality, is actually equivalent to the non-separability of the state [13, 44] whose conditions has been computed in Eq. (29).

We now compare the three different criteria for deciding whether a system behaves quantum-mechanically or not: the quantum discord (15), the violation of Bell inequalities (27) and the non-separability of the state (29). As mentioned above, the squeezing angle φ can be adjusted by rotating the measurement direction in phase space. This is why, for the Bell inequality (27), which is the only criterion depending on φ, we choose to optimise φ in order to get the maximal violation. It corresponds to setting $\varphi = 0$. All three criteria thus depend on r and p only, and are shown in Fig. 2. The colour encodes the value of quantum discord as given by Eq. (15), the black dashed line corresponds to the threshold for Bell-inequality violation, Eq. (27), while the white line stands for the non-separability criterion as given in Eq. (29).

One can check that, for pure state ($p = 1$), all criteria are equivalent: except from the vacuum state ($r = 0$), all states have non-vanishing quantum discord, are non separable and violate the Bell inequality. In this sense, for a pure Gaussian state, any correlation is quantum in nature. For mixed states ($p < 1$), non-separability is a necessary but non-sufficient condition for the Bell-inequality violation [81] (i.e. the white line is below the black line), and non-discordant states are separable [11] (i.e. the dark blue region is below

the white line).

These results also confirm that decoherence (i.e. smaller value for p) is associated to the emergence of classicality. Indeed, for a given squeezing amplitude r, there always exists a value of the purity parameter p below which the Bell inequality is not violated, the state is separable and quantum discord is smaller than a given threshold. The required amount of decoherence (i.e. the critical value for the purity parameter p), increases (decreases) with the squeezing amplitude. This is because, as r increases, the two subsystems get more entangled, hence it takes more decoherence to erase quantum features. In [48], the authors had considered a similar class of states and studied the robustness of non-classicality measures against decoherence induced by coupling to thermal baths. In this special case it was also found that the state becomes classical in the sense that quantum discord asymptotes zero at large decoherence, and that separability vanishes once decoherence reaches a certain finite threshold.

Our findings also prompt some reservations about the physical relevance of the numerical value of quantum discord. Discord is measured in information bits and, a priori, one may think that it is an extensive quantity, namely the larger the discord the more "quantum" the state. However, one notices in Fig. 2 that the value of quantum discord at which the separability or Bell criteria are crossed may be small or large, depending on the squeezing amplitude. For instance, if the state is almost pure $p \sim 1$ and the squeezing weak $r \leq 1$, then one can achieve a non-separable state and/or a Bell inequality violation while keeping a small quantum discord, see point "A"; or for large squeezing and small purity we can both have a large quantum discord and still satisfy the Bell inequality, see point "B". This suggests that the numerical value of discord itself has no clear interpretation, at least in this setup and in terms of the other quantumness criteria.

The behaviour of these three criteria can be further understood in the phase-space representation. Ignoring the orientation φ (which we have set to its optimal value $\varphi = 0$ for Bell inequality violation), the ellipses of Fig. 1 have been parameterised so far using their area, via p, and their eccentricity, via r. Alternatively, one can describe them by means of their semi-major, a, and semi-minor, b, axes, related to r and p by

$$a = e^r p^{-1/4}, \quad b = e^{-r} p^{-1/4}. \tag{30}$$

In particular, we expect b, the size of semi-minor axis, to play a physical role since it encodes the presence or absence of a sub-fluctuant direction in phase space with respect to the vacuum.

Using Eq. (30) all criteria can be expressed in terms of a and b. The non-separability criterion assumes an extremely simple form as Eq. (29) is straightforwardly recast to $b \geq 1$. The fact that the state is non-separable is then equivalent to the existence of a sub-fluctuant direction in phase space (for instance, in Fig. 1 the state represented by the green ellipse is non-separable while the one represented by the blue ellipse is separable). The expression of quantum discord and the Bell operator in terms of a and b is not particularly illuminating but in the large-squeezing and small-purity limit, i.e. $a \gg b \gg 1/a$, in the appendix we show that the discord also becomes a function of b only (i.e. of the sub-fluctuant mode), namely

$$\mathcal{D}(a,b) \to g\left(1+2b^2\right) + \log_2\left(1+\frac{1}{2b^2}\right), \tag{31}$$

where $g(x)$ is bounded and defined in Eq. (64).

All criteria are displayed as a function of a and b in Fig. 3, where one can check that $\langle \hat{B} \rangle$ and $\mathcal{D}$ become independent of a in the large-squeezing limit.

Conclusions. – In this letter, we compared three different criteria, quantum discord, Bell inequality violation and non-separability, aimed at assessing whether a system behaves quantum-mechanically or not. We have found that, even in a simple class of Gaussian states, these criteria are inequivalent, i.e. a state can be, at the same time, "quantum" according to one criterion and "classical" according to another one. However,

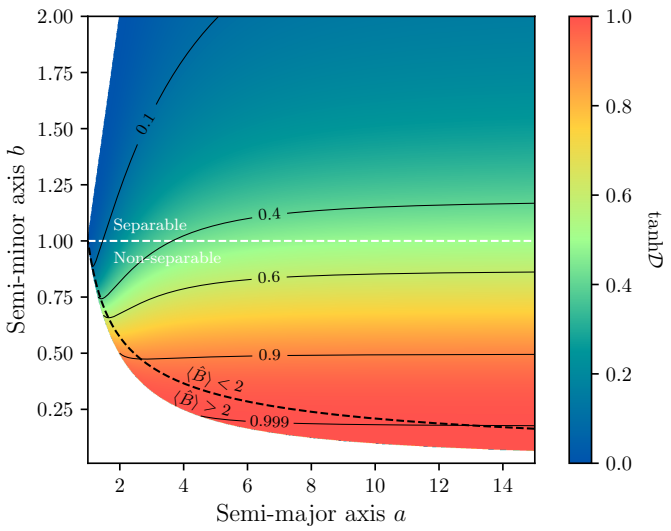

Fig. 3: Same criteria as in Fig. 2, as a function of the semi-major a and semi-minor b axes of the phase-space ellipses depicted in Fig. 1. The solid black lines are contour levels of quantum discord. The white region corresponds to either $a < b$ or $p > 1$, which are both non physical. In the large squeezing limit, $b \ll a$, $\langle\hat{B}\rangle = 2$ (black dashed line) is equivalent to $b = [\pi/(8a^3)]^{1/5}$.

in the large squeezing limit these criteria were found to be mainly controlled by the amplitude of the sub-fluctuant mode. There is no natural threshold for the value of quantum discord at which the other two criteria are crossed, and we found that decoherence always leads to more classical states regardless of the criterion being used.

This analysis could be extended to non-Gaussian states [79], which are known to behave differently under quantum criteria (for instance, according to Hudson theorem [39] their Wigner functions are necessarily non-positive if they are pure).

* * *

We thank Scott Robertson for interesting discussions and useful suggestions. A. Micheli is supported by the French National Research Agency under the Grant No. ANR-20-CE47-0001 associated with the project COSQUA.

REFERENCES

[1] Gerardo Adesso and Animesh Datta. Quantum versus Classical Correlations in Gaussian States. *Physical Review Letters*, 105(3):030501, July 2010.

[2] Gerardo Adesso, Sammy Ragy, and Antony R. Lee. Continuous variable quantum information: Gaussian states and beyond. *Open Systems & Information Dynamics*, 21(01n02):1440001, June 2014.

[3] Ivan Agullo, Béatrice Bonga, and Patricia Ribes Metidieri. Does inflation squeeze cosmological perturbations? *arXiv:2203.07066*, March 2022.

[4] Ivan Agullo, Anthony J. Brady, and Dimitrios Kranas. Event horizons are tunable factories of quantum entanglement. 9 2022.

[5] Andreas Albrecht and Paul J. Steinhardt. Cosmology for Grand Unified Theories with Radiatively Induced Symmetry Breaking. *Phys. Rev. Lett.*, 48:1220–1223, 1982.

[6] Konrad Banaszek and Krzysztof Wodkiewicz. Quantum Nonlocality in Phase Space. *Physical Review Letters*, 82(10):2009–2013, March 1999.

[7] Shreya Banerjee, Sayantani Bera, and Tejinder P. Singh. Quantum discord as a tool for comparing collapse models and decoherence. *Physics Letters A*, 380(45):3778–3785, November 2016.

[8] James M. Bardeen, Paul J. Steinhardt, and Michael S. Turner. Spontaneous Creation of Almost Scale - Free Density Perturbations in an Inflationary Universe. *Phys. Rev. D*, 28:679, 1983.

[9] S. M. Barnett and P. M. Radmore. *Methods in Theoretical Quantum Optics*. Clarendon Press Publication, Oxford, 1997.

[10] J. S. Bell. On the Einstein Podolsky Rosen paradox. *Physics Physique Fizika*, 1(3):195–200, November 1964.

[11] Anindita Bera, Tamoghna Das, Debasis Sadhukhan, Sudipto Singha Roy, Aditi Sen De, and Ujjwal Sen. Quantum discord and its allies: A review. *Reports on Progress in Physics*, 81(2):024001, February 2018.

[12] Xavier Busch, Renaud Parentani, and Scott Robertson. Quantum entanglement due to a modulated dynamical Casimir effect. *Phys. Rev. A*, 89(6):063606, 2014.

[13] David Campo and Renaud Parentani. Inflationary spectra and partially decohered distributions. *Physical Review D*, 72(4):045015, August 2005.

[14] David Campo and Renaud Parentani. Inflationary spectra and violations of Bell inequalities. *Physical Review D*, 74(2):025001, July 2006.

[15] David Campo and Renaud Parentani. Decoherence and entropy of primordial fluctuations. I. Formalism and interpretation. *Physical Review D*, 78(6):065044, September 2008.

[16] William B. Case. Wigner functions and Weyl transforms for pedestrians. *American Journal of Physics*, 76(10):937–946, October 2008.

[17] Carlton M. Caves and Bonny L. Schumaker. New formalism for two-photon quantum optics. 1. Quadrature phases and squeezed states. *Phys. Rev.*, A31:3068–3092, 1985.

[18] John F. Clauser, Michael A. Horne, Abner Shimony, and Richard A. Holt. Proposed Experiment to Test Local Hidden-Variable Theories. *Physical Review Letters*, 23(15):880–884, October 1969.

[19] Thomas Colas, Julien Grain, and Vincent Vennin. Four-mode squeezed states: two-field quantum systems and the symplectic group $\mathrm{Sp}(4,\mathbb{R})$. *Eur. Phys. J. C*, 82(1):6, 2022.

[20] Planck Collaboration. Planck 2018 results. X: Constraints on inflation. *Astronomy & Astrophysics*, 641:A10, September 2020.

[21] Artur K. Ekert. Quantum cryptography based on Bell's theorem. *Physical Review Letters*, 67(6):661–663, August 1991.

[22] J. Estève, C. Gross, A. Weller, S. Giovanazzi, and M. K. Oberthaler. Squeezing and entanglement in a Bose-Einstein condensate. *Nature*, 455(7217):1216–1219, October 2008.

[23] Alessandro Ferraro, Stefano Olivares, and Matteo G. A. Paris. Gaussian states in continuous variable quantum information, March 2005.

[24] Alessandro Ferraro and Matteo G. A. Paris. Nonclassicality Criteria from Phase-Space Representations and Information-Theoretical Constraints Are Maximally Inequivalent. *Physical Review Letters*, 108(26):260403, June 2012.

[25] Marco G. Genoni, Ludovico Lami, and Alessio Serafini. Conditional and unconditional Gaussian quantum dynamics. *Contemporary Physics*, 57(3):331–349, July 2016.

[26] Marco G. Genoni, Mattia L. Palma, Tommaso Tufarelli, Stefano Olivares, M. S. Kim, and Matteo G. A. Paris. Detecting quantum non-Gaussianity via the Wigner function. *Phys. Rev. A*, 87(6):062104, June 2013.

[27] Paolo Giorda and Matteo G. A. Paris. Gaussian Quantum Discord. *Physical Review Letters*, 105(2):020503, July 2010.

[28] Roy J. Glauber. Coherent and Incoherent States of the Radiation Field. *Physical Review*, 131(6):2766–2788, September 1963.

[29] G. Gour, F. C. Khanna, A. Mann, and M. Revzen. Optimization of Bell's Inequality Violation For Continuous Variable Systems. *Physics Letters A*, 324(5-6):415–419, April 2004.

[30] Julien Grain and Vincent Vennin. Canonical transformations and squeezing formalism in cosmology. *Journal of Cosmology and Astroparticle Physics*, 2020(02):022–022, February 2020.

[31] L. P. Grishchuk and Y. V. Sidorov. Squeezed quantum states of relic gravitons and primordial density fluctuations. *Physical Review D*, 42(10):3413–3421, November 1990.

[32] Alan H. Guth. The Inflationary Universe: A Possible Solution to the Horizon and Flatness

Problems. *Phys. Rev. D*, 23:347–356, 1981.

[33] Alan H. Guth and S. Y. Pi. Fluctuations in the New Inflationary Universe. *Phys. Rev. Lett.*, 49:1110–1113, 1982.

[34] S. W. Hawking. Particle Creation by Black Holes. *Commun. Math. Phys.*, 43:199–220, 1975. [Erratum: Commun.Math.Phys. 46, 206 (1976)].

[35] S. W. Hawking. The Development of Irregularities in a Single Bubble Inflationary Universe. *Phys. Lett. B*, 115:295, 1982.

[36] L. Henderson and V. Vedral. Classical, quantum and total correlations. 2001.

[37] Michal Horodecki, Pawel Horodecki, and Ryszard Horodecki. On the necessary and sufficient conditions for separability of mixed quantum states. *Phys. Lett. A*, 223:1, 1996.

[38] Ryszard Horodecki, Paweł Horodecki, Michał Horodecki, and Karol Horodecki. Quantum entanglement. *Reviews of Modern Physics*, 81(2):865–942, June 2009.

[39] R.L. Hudson. When is the wigner quasi-probability density non-negative? *Reports on Mathematical Physics*, 6(2):249–252, 1974.

[40] J.-C. Jaskula, G. B. Partridge, M. Bonneau, R. Lopes, J. Ruaudel, D. Boiron, and C. I. Westbrook. Acoustic Analog to the Dynamical Casimir Effect in a Bose-Einstein Condensate. *Physical Review Letters*, 109(22):220401, November 2012.

[41] Hyunseok Jeong, Jinhyoung Lee, and M. S. Kim. Dynamics of Nonlocality for A Two-Mode Squeezed State in Thermal Environment. *Physical Review A*, 61(5):052101, March 2000.

[42] E. Joos and H. D. Zeh. The Emergence of classical properties through interaction with the environment. *Z. Phys. B*, 59:223–243, 1985.

[43] Richard Jozsa and Noah Linden. On the role of entanglement in quantum computational speed-up. *Proceedings of the Royal Society of London. Series A: Mathematical, Physical and Engineering Sciences*, 459(2036):2011–2032, August 2003.

[44] M. S. Kim, F. A. M. de Oliveira, and P. L. Knight. Properties of squeezed number states and squeezed thermal states. *Physical Review A*, 40(5):2494–2503, September 1989.

[45] J. Lesgourgues, David Polarski, and Alexei A. Starobinsky. Quantum to classical transition of cosmological perturbations for nonvacuum initial states. *Nucl. Phys. B*, 497:479–510, 1997.

[46] Andrei D. Linde. A New Inflationary Universe Scenario: A Possible Solution of the Horizon, Flatness, Homogeneity, Isotropy and Primordial Monopole Problems. *Phys. Lett. B*, 108:389–393, 1982.

[47] Andrei D. Linde. Chaotic Inflation. *Phys. Lett. B*, 129:177–181, 1983.

[48] Paulina Marian, Iulia Ghiu, and Tudor A Marian. Decay of Gaussian correlations in local thermal reservoirs. *Physica Scripta*, 90(7):074041, June 2015.

[49] Jérôme Martin. Cosmic Inflation, Quantum Information and the Pioneering Role of John S Bell in Cosmology. *Universe*, 5(4):92, April 2019.

[50] Jérôme Martin, Amaury Micheli, and Vincent Vennin. Discord and decoherence. *Journal of Cosmology and Astroparticle Physics*, 2022(04):051, April 2022.

[51] Jerome Martin and Vincent Vennin. Quantum Discord of Cosmic Inflation: Can we Show that CMB Anisotropies are of Quantum-Mechanical Origin? *Phys. Rev. D*, 93(2):023505, 2016.

[52] Jérôme Martin and Vincent Vennin. Quantum discord of cosmic inflation: Can we show that CMB anisotropies are of quantum-mechanical origin? *Physical Review D*, 93(2):023505, January 2016.

[53] Jerome Martin and Vincent Vennin. Obstructions to Bell CMB Experiments. *Phys. Rev. D*, 96(6):063501, 2017.

[54] Jerome Martin and Vincent Vennin. Obstructions to Bell CMB Experiments. *Physical Review D*, 96(6):063501, September 2017.

[55] Jérôme Martin and Vincent Vennin. Cosmic Microwave Background Constraints Cast a Shadow On Continuous Spontaneous Localization Models. *Phys. Rev. Lett.*, 124(8):080402, 2020.

[56] Jerome Martin and Vincent Vennin. Real-space entanglement in the Cosmic Microwave Background. *Journal of Cosmology and Astroparticle Physics*, 2021(10):036, October 2021.

[57] Jerome Martin and Vincent Vennin. Real-space entanglement of quantum fields. *Physical Review D*, 104(8):085012, October 2021.

[58] Tim Maudlin. What Bell did. *Journal of Physics A: Mathematical and Theoretical*, 47(42):424010, October 2014.

[59] Amaury Micheli and Patrick Peter. Quantum cosmological gravitational waves?, November 2022.

[60] Viatcheslav F. Mukhanov and G. V. Chibisov. Quantum Fluctuations and a Nonsingular Universe. *JETP Lett.*, 33:532–535, 1981.

[61] Viatcheslav F. Mukhanov and G. V. Chibisov. The Vacuum energy and large scale structure of the universe. *Sov. Phys. JETP*, 56:258–265, 1982.

[62] A. Nunnenkamp, K. Børkje, J. G. E. Harris, and S. M. Girvin. Cooling and squeezing via quadratic optomechanical coupling. *Phys. Rev. A*, 82(2):021806, August 2010.

[63] Harold Ollivier and Wojciech H. Zurek. Quantum Discord: A Measure of the Quantumness of Correlations. *Phys. Rev. Lett.*, 88:017901, 2001.

[64] Nelson Pinto-Neto, Grasiele Santos, and Ward Struyve. Quantum-to-classical transition of primordial cosmological perturbations in de Broglie–Bohm quantum theory. *Phys. Rev. D*, 85:083506, 2012.

[65] Stefano Pirandola, Gaetana Spedalieri, Samuel L. Braunstein, Nicolas J. Cerf, and Seth Lloyd. Optimality of Gaussian Discord. *Physical Review Letters*, 113(14):140405, October 2014.

[66] S. Pironio, A. Acín, S. Massar, A. Boyer de la Giroday, D. N. Matsukevich, P. Maunz, S. Olmschenk, D. Hayes, L. Luo, T. A. Manning, and C. Monroe. Random numbers certified by Bell's theorem. *Nature*, 464(7291):1021–1024, April 2010.

[67] M. Revzen, P. A. Mello, A. Mann, and L. M. Johansen. Bell's Inequality Violation (BIQV) with Non-Negative Wigner Function. *Physical Review A*, 71(2):022103, February 2005.

[68] Scott Robertson, Florent Michel, and Renaud Parentani. Assessing degrees of entanglement of phonon states in atomic Bose gases through the measurement of commuting observables. *Physical Review D*, 96(4):045012, August 2017.

[69] K. Sato. First Order Phase Transition of a Vacuum and Expansion of the Universe. *Mon. Not. Roy. Astron. Soc.*, 195:467–479, 1981.

[70] Bonny L. Schumaker and Carlton M. Caves. New formalism for two-photon quantum optics. 2. Mathematical foundation and compact notation. *Phys. Rev.*, A31:3093–3111, 1985.

[71] Alessio Serafini, Fabrizio Illuminati, Matteo G. A. Paris, and Silvio De Siena. Entanglement and purity of two-mode Gaussian states in noisy channels. *Physical Review A*, 69(2):022318, February 2004.

[72] R. Simon. Peres-Horodecki separability criterion for continuous variable systems. *Physical Review Letters*, 84(12):2726–2729, March 2000.

[73] R. Simon, E.C.G. Sudarshan, and N. Mukunda. Gaussian wigner distributions: A complete characterization. *Physics Letters A*, 124(4):223 – 228, 1987.

[74] Alexei A. Starobinsky. A New Type of Isotropic Cosmological Models Without Singularity. *Phys. Lett. B*, 91:99–102, 1980.

[75] Alexei A. Starobinsky. Dynamics of Phase Transition in the New Inflationary Universe Scenario and Generation of Perturbations. *Phys. Lett. B*, 117:175–178, 1982.

[76] Jeff Steinhauer. Observation of quantum Hawking radiation and its entanglement in an analogue black hole. *Nature Physics*, 12(10):959–965, October 2016.

[77] E. C. G. Sudarshan. Equivalence of Semiclassical and Quantum Mechanical Descriptions of Statistical Light Beams. *Physical Review Letters*, 10(7):277–279, April 1963.

[78] Daniel Sudarsky. Shortcomings in the Understanding of Why Cosmological Perturbations Look Classical. *Int. J. Mod. Phys. D*, 20:509–552, 2011.

[79] Mattia Walschaers. Non-Gaussian Quantum States and Where to Find Them. *PRX Quantum*, 2(3):030204, September 2021.

[80] J. Weinbub and D. K. Ferry. Recent advances in Wigner function approaches. *Applied Physics Reviews*, 5(4):041104, December 2018.

[81] Reinhard F. Werner. Quantum states with Einstein-Podolsky-Rosen correlations admitting a hidden-variable model. *Physical Review A*, 40(8):4277–4281, October 1989.

[82] Eugene P. Wigner. On the quantum correction for thermodynamic equilibrium. *Phys. Rev.*, 40:749–760, 1932.

[83] H. M. Wiseman, S. J. Jones, and A. C. Doherty. Steering, Entanglement, Nonlocality, and the EPR Paradox. *Physical Review Letters*, 98(14):140402, April 2007.

[84] W. H. Zurek. Pointer Basis of Quantum Apparatus: Into What Mixture Does the Wave

Packet Collapse? *Phys. Rev. D*, 24:1516–1525, 1981.

[85] W. H. Zurek. Environment induced superselection rules. *Phys. Rev. D*, 26:1862–1880, 1982.

Appendix. – In the two first sections of this appendix we present the technical details relevant for computing the expectation value of the Bell operator and the separability criterion for Gaussian states. In the third section, we show that, in the limit $r \gg 1$ and $p \ll 1$, quantum discord is only controlled by b, the size of the semi-minor axis introduced in the main text. In the last section we analyse the effect of two specific Gaussian noisy channels, namely the pure-loss and the additive-noise channels, on the non-classicality of a TMSV using the criteria identified in the text.

Weyl transform of spin operators and expectation value of Bell operator. We start by presenting the computation of the Weyl transform of the spin operators defined in Eq. (18). The Weyl transform of an operator has been defined in Eq. (1). We apply this formula to $\hat{\sigma}_z^i$, the spin operator of the $i^{\rm rm}$ subsystem along z

$$\widetilde{\sigma_z^i}\left(q_i,p_i\right) = \int_{-\infty}^{\infty} e^{ip_i y}\left\langle q_i+\frac{y}{2}\right|\left(-\int_{-\infty}^{\infty}\left|x\right\rangle\left\langle -x\right|\mathrm{d}x\right)\left|q_i-\frac{y}{2}\right\rangle \mathrm{d}y \tag{32}$$

$$= -\int_{-\infty}^{\infty} e^{ip_i y}\int_{-\infty}^{\infty}\delta\left(q_i+\frac{y}{2}-x\right)\delta\left(q_i-\frac{y}{2}+x\right)\mathrm{d}x\,\mathrm{d}y \tag{33}$$

$$= -\delta\left(2q_i\right)\int_{-\infty}^{\infty} e^{ip_i y}\mathrm{d}y \tag{34}$$

$$= -\pi\delta\left(q_i\right)\delta\left(p_i\right)\,, \tag{35}$$

which is the formula given in Eq. (24). This readily gives Eq. (25). Proceeding similarly for the spin operator along x we get

$$\widetilde{\sigma_x^i}\left(q_i,p_i\right) = \int_{-\infty}^{\infty} e^{ip_i y}\left\langle q_i+\frac{y}{2}\right|\left(-\int_{-\infty}^{\infty}\mathrm{sign}\left(x\right)\left|x\right\rangle\left\langle -x\right|\mathrm{d}x\right)\left|q_i-\frac{y}{2}\right\rangle \mathrm{d}y \tag{36}$$

$$= \int_{-\infty}^{\infty} e^{ip_i y}\int_{-\infty}^{\infty}\mathrm{sign}\left(x\right)\delta\left(q_i+\frac{y}{2}-x\right)\delta\left(x-q_i+\frac{y}{2}\right)\mathrm{d}x\,\mathrm{d}y \tag{37}$$

$$= \int_{-\infty}^{\infty} e^{ip_i y}\,\mathrm{sign}\left(q_i-\frac{y}{2}\right)\delta\left(y\right)\mathrm{d}y \tag{38}$$

$$= \mathrm{sign}\left(q_i\right)\,, \tag{39}$$

which is the (second) formula given in Eq (24). Using Eq. (2) and the Gaussian Wigner function (4), the expectation value of $\hat{\sigma}_z^1\hat{\sigma}_z^2$ can then be obtained as

$$\left\langle\hat{\sigma}_x^1\hat{\sigma}_x^2\right\rangle = \int\frac{\mathrm{sign}\left(q_1\right)\mathrm{sign}\left(q_2\right)}{\pi^2\sqrt{\det\gamma}}\exp\left(-R_{1/2}^{\rm T}\gamma^{-1}R_{1/2}\right)\mathrm{d}q_1\,\mathrm{d}p_1\,\mathrm{d}q_2\,\mathrm{d}p_2 \tag{40}$$

$$= \int\frac{\mathrm{sign}\left(q_1\right)\mathrm{sign}\left(q_2\right)}{\pi\sqrt{\gamma_{qq}\gamma_{pp}}}\exp\left[-\frac{\left(q_1+q_2\right)^2}{2\gamma_{qq}}-\frac{\left(q_1-q_2\right)^2}{2\gamma_{pp}}\right]\mathrm{d}q_1\,\mathrm{d}q_2 \tag{41}$$

$$= -\frac{2}{\pi}\arctan\left[\frac{\cos(2\varphi)\sinh(2r)}{\sqrt{1+\sin^2\left(2\varphi\right)\sinh\left(2r\right)}}\right] \tag{42}$$

$$= -\frac{2}{\pi}\arcsin\left[\left|\cos(2\varphi)\right|\tanh(2r)\right]\,, \tag{43}$$

where in the second line we have performed the integration over p_1 and p_2, and in the third line over q_1 and q_2 after having inserted the expression of γ_{qq} and γ_{pp} given by Eqs.(12) and (14). The last result is nothing but Eq. (26).

Separability criterion. In this section we derive Eq. (29) of the main text, i.e. the condition for a Gaussian state to be separable. In the partition leading to Eq. (9), the result is known, see for instance [15]. Here we extend this result to the one-parameter family of partitions considered in Ref. [50]: starting from $\hat{\boldsymbol{R}}_{\rm D}$, it is obtained by performing the canonical transformation $\hat{\boldsymbol{R}}_{\rm D} \to S(\theta)\hat{\boldsymbol{R}}_{\rm D}$ where $S(\theta)$ is the symplectic matrix

$$S\left(\theta\right) = \begin{pmatrix} \cos\theta & 0 & 0 & \sin\theta \\ 0 & \cos\theta & -\sin\theta & 0 \\ \sin\theta\sin(2\theta) & \sin\theta\cos(2\theta) & \cos\theta\cos(2\theta) & -\cos\theta\sin(2\theta) \\ -\sin\theta\cos(2\theta) & \sin\theta\sin(2\theta) & \cos\theta\sin(2\theta) & \cos\theta\cos(2\theta) \end{pmatrix}. \tag{44}$$

This class of partitions is parameterised by the angle θ. The partition (9) corresponds to $\theta = -\pi/4$, while the factorised partition, i.e. the one leading to Eq. (10), corresponds to $\theta = 0$. For arbitrary θ the covariance matrix reads

$$\gamma = \begin{pmatrix} \gamma_A & \gamma_C \\ \gamma_C & \gamma_B \end{pmatrix}, \tag{45}$$

with

$$\gamma_A = \begin{pmatrix} \gamma_{11}\cos^2\theta + \gamma_{22}\sin^2\theta & \gamma_{12}\cos(2\theta) \\ \gamma_{12}\cos(2\theta) & \gamma_{22}\cos^2\theta + \gamma_{11}\sin^2\theta \end{pmatrix}, \tag{46}$$

$$\gamma_B = \begin{pmatrix} \gamma_B|_{11} & \gamma_B|_{12} \\ \gamma_B|_{21} & \gamma_B|_{22} \end{pmatrix}, \tag{47}$$

$$\gamma_C = \begin{pmatrix} \frac{1}{2}(\gamma_{11}-\gamma_{22})\sin^2(2\theta) + \frac{1}{2}\gamma_{12}\sin(4\theta) & -\frac{1}{4}(\gamma_{11}-\gamma_{22})\sin(4\theta) + \gamma_{12}\sin^2(2\theta) \\ -\frac{1}{4}(\gamma_{11}-\gamma_{22})\sin(4\theta) + \gamma_{12}\sin^2(2\theta) & -\frac{1}{2}(\gamma_{11}-\gamma_{22})\sin^2(2\theta) - \frac{1}{2}\gamma_{12}\sin(4\theta) \end{pmatrix}, \tag{48}$$

and where the components of γ_B are given by

$$\gamma_B|_{11} = \frac{1}{2}\gamma_{11} + \frac{1}{2}\gamma_{22} + \frac{1}{2}(\gamma_{11}-\gamma_{22})\cos(2\theta)\cos(4\theta) - \gamma_{12}\cos(2\theta)\sin(4\theta), \tag{49}$$

$$\gamma_B|_{12} = \gamma_B|_{21} = \gamma_{12}\cos(2\theta)\cos(4\theta) + \frac{1}{2}(\gamma_{11}-\gamma_{22})\cos(2\theta)\sin(4\theta), \tag{50}$$

$$\gamma_B|_{22} = \frac{1}{2}\gamma_{11} + \frac{1}{2}\gamma_{22} - \frac{1}{2}(\gamma_{11}-\gamma_{22})\cos(2\theta)\cos(4\theta) + \gamma_{12}\cos(2\theta)\sin(4\theta). \tag{51}$$

For a general covariance matrix the Peres-Horodecki criterion for separability can be written as [73]

$$\det\gamma_A\det\gamma_B + \left(|\det\gamma_C| - 1\right)^2 - \mathrm{Tr}\left[\gamma_A J^{(1)}\gamma_C J^{(1)}\gamma_B J^{(1)}\gamma_C^{\rm T} J^{(1)}\right] \geq \det\gamma_A + \det\gamma_B\,, \tag{52}$$

where the matrix $J^{(1)}$ is defined by $J^{(1)} \equiv \begin{pmatrix} 0 & 1 \\ -1 & 0 \end{pmatrix}$. Using the above expressions, straightforward

manipulations lead to

$$\det\gamma_A = \det\gamma_B = \frac{1}{p}\left[\cosh^2(2r) - \cos^2(2\theta)\sinh^2(2r)\right] = \frac{1}{p} - \det\gamma_C, \tag{53}$$

$$\det\gamma_C = -\frac{1}{p}\sinh^2(2r)\sin^2(2\theta), \tag{54}$$

$$\mathrm{Tr}\left[\gamma_A J^{(1)}\gamma_C J^{(1)}\gamma_B J^{(1)}\gamma_C^{\mathrm{T}} J^{(1)}\right] = -2\det\gamma_C\left(\frac{1}{p} - \det\gamma_C\right). \tag{55}$$

Combining the above results, the general criterion (52) can be written as a condition on $\det(\gamma_C)$ only, which is always negative as can be seen in Eq. (54). One obtains

$$\left(\frac{1}{p} - \det\gamma_C\right)^2 + (\det\gamma_C + 1)^2 + 2\det\gamma_C\left(\frac{1}{p} - \det\gamma_C\right) \geq 2\left(\frac{1}{p} - \det\gamma_C\right). \tag{56}$$

Using Eq. (54) the above reduces to

$$\frac{1}{p^2} - \frac{2}{p} + 1 + 4\det\gamma_C \geq 0\,. \tag{57}$$

Using Eq. (54) again, one finds

$$\left(\frac{1}{\sqrt{p}} - \sqrt{p}\right)^2 \geq 4\sinh^2(2r)\sin^2(2\theta)\,. \tag{58}$$

In the partition leading to Eq. (9), the above expression can be evaluated with $\theta = -\pi/4$, a value for which the previous formula reduces to

$$\left(\frac{1}{\sqrt{p}} - \sqrt{p}\right)^2 \geq \left(\frac{1}{e^{-2r}} - e^{-2r}\right)^2. \tag{59}$$

Given that both $\sqrt{p}$ and e^{-2r} are smaller than one, and since $y \to y - 1/y$ is a strictly increasing function, this finally leads to

$$\frac{e^{-2r}}{\sqrt{p}} \geq 1\,, \tag{60}$$

which corresponds to Eq. (29).

Quantum discord in the large-squeezing limit. Using Eqs. (30), we can re-write the expression (15) of the quantum discord in terms of the lengths of the semi-major, a, and semi-minor axis, b. Eq. (15) only depends on the quantity σ, defined by Eq. (17), and p. Therefore, we need to express these two quantities in terms of a and b and one obtains

$$\sigma = \frac{1}{2}\left(a^2 + b^2\right), \quad p = \frac{1}{a^2 b^2}. \tag{61}$$

Combining Eq. (15) and the two above formula, we get the following expression for the quantum discord as a function of a and b only

$$\mathcal{D}(a,b) = f\left[\frac{1}{2}\left(a^2 + b^2\right)\right] - 2f\left(ab\right) + f\left(\frac{a^2 + b^2 + 2a^2b^2}{a^2 + b^2 + 2}\right). \tag{62}$$

Under this form the quantum discord is expressed as a sum of terms which have no definite sign and are unbounded. In order to see that $\mathcal{D}$ is only controlled by b in the large-squeezing (i.e. $a \gg b$) and small-purity (i.e. $ab = 1/\sqrt{p} \gg 1$) limit, we rewrite the above as

$$\mathcal{D}(a,b) = g\left[\frac{1}{2}\left(a^2+b^2\right)\right] - 2g\left(ab\right) + g\left(\frac{a^2+b^2+2a^2b^2}{a^2+b^2+2}\right) + \log_2\left[\frac{(a^2+b^2)(a^2+b^2+2a^2b^2)}{2a^2b^2(a^2+b^2+2)}\right], \quad (63)$$

where we have defined the function $g(x)$ by

$$g(x) = f(x) - \log_2\left(\frac{x}{2}\right) - \frac{1}{\ln 2}. \quad (64)$$

The function $g(x)$ is defined as the difference between $f(x)$ and its asymptotic value at large argument. One can check that $g(x)$ is a negative, strictly increasing function, which is bounded by its limits $\lim_{x\to 1^+} g(x) = -1/\ln 2 + 1 \approx -0.44$ and $\lim_{x\to+\infty} g(x) = 0$. The large-squeezing regime corresponds to $b \gg a$. Since $ab \geq 1$ for the purity to be smaller than one, large squeezing requires $a \gg 1$, i.e. the semi-major axis must be much larger than its vacuum value. The first term in Eq. (63) therefore vanishes in this limit. In addition, for small purity $ab = 1/\sqrt{p} \gg 1$, the second term vanishes as well. We are thus left with the last two terms, which, in this limit, read

$$\mathcal{D}(a,b) \to g\left(1+2b^2\right) + \log_2\left(1+\frac{1}{2b^2}\right). \quad (65)$$

Therefore, the value of the discord only depends on the size of the semi-minor axis b as can be seen in the lower-right corner of Fig. 3. Note that asymptotic expression behaves as expected in the limit of a large semi-minor axis, $b \gg 1$, where $\mathcal{D}$ goes to 0. In the opposite limit, namely, $b \ll 1$, the first term goes to a finite value while the second one vanishes.

Pure-loss and additive-noise channels. Consider now the effect of a pure-loss channel of efficiency η on a TMSV whose covariance matrix is given by Eq. (6). The resulting covariance matrix, $\eta\boldsymbol{\gamma}^{\mathrm{TMSV}} + (1-\eta)\,\mathbb{1}_4$, can be recast in the form of Eq. (9) using the following effective squeezing parameters and purity

$$r' = \frac{1}{2}\mathrm{arctanh}\left[\frac{\eta\sinh(2r)}{\eta\cosh(2r)+1-\eta}\right], \quad \varphi' = \varphi, \quad p = \frac{1}{1+4\sinh^2(r)\,\eta\,(1-\eta)}. \quad (66)$$

We check that, in the limit $\eta \to 1$ (no loss), the rescaled squeezing parameters coincide with the original ones and $p = 1$. Using this mapping we can express the quantum discord, the non-separability and the Bell violation criteria with the help of the formulas derived in the main text. We plot these three criteria in Fig. 4, where we set $\varphi = 0$ to optimise for the violation of the Bell inequality.

First, we notice that, at fixed value of r, the discord increases with η, which is intuitive since we expect the quantumness of the state to be more and more preserved as the loss decreases. Of course, on the other hand, at fixed efficiency, the discord increases as r increases.

Second, the criterion for separability (52), expressed in terms of r and η, reads

$$-16\eta^2\sinh^2(r)\left[1+\eta\,(2-\eta)\sinh^2(r)\right] \geq 0, \quad (67)$$

which can only be satisfied if $r = 0$. This means that, after having gone through the loss channel, an initial non-separable state will always remain non-separable irrespective of its efficiency as expected for such pure damping [71].

Third, in Fig. 4, we have also represented the threshold for violation of Bell inequality, see the black dashed line. In terms of r and η, it is given by the following expression,

$$\langle \hat{B} \rangle = 2\sqrt{\frac{1}{\left[1+4\sinh^2(r)\,\eta\,(1-\eta)\right]^2} + \frac{4}{\pi^2}\arcsin^2\left[\frac{\eta\sinh(2r)}{\eta\cosh(2r)+1-\eta}\right]}\,, \tag{68}$$

This threshold is discontinuous at $r = 0$. Indeed, for $r = 0$, the system is in the vacuum which does not violate the Bell inequality $\left\langle \hat{B} \right\rangle = 2$. For small but non-vanishing value of the squeezing parameter, we can expand the expression of $\langle \hat{B} \rangle$,

$$\langle \hat{B} \rangle \sim 2 + 8r^2\eta\left[\left(\frac{2}{\pi^2}+1\right)\eta - 1\right]\,, \tag{69}$$

and, as a consequence, the threshold of violation for the Bell inequality corresponds to $\eta \geq \left(1+2\pi^{-2}\right)^{-1} \sim 0.83$, which is independent of the squeezing parameter r. We now consider the large r behaviour of the threshold. The figure shows that for large initial squeezing the level of loss required to prevent the violation of the Bell inequality *decreases*. This is consistent with the results of [41] where the authors consider a TMSV interacting with two thermal baths, and showed that the violation of the Bell inequality considered in [6] decreases with the initial squeezing. Since a large squeezing also implies stronger correlation, and larger value of the Bell operator initially, this fact might appear surprising at first. However, this picture overlooks that the decoherence caused this pure-channel is more efficient for strongly squeezed states. Indeed, Eq. (66) shows that for a channel with fixed efficiency η, increasing the initial squeezing r of the TMSV will exponentially suppress its purity p after the channel. This decoherence is suppressing the first term in Eq. (68), while the stronger correlation increase the second term. The fact that the threshold of Bell inequality violation goes to $\eta = 1$ shows that this increase is not sufficient to compensate the decoherence encoded in the first term. We can check this behaviour by approximating the curve $\langle \hat{B} \rangle = 2$ in the vicinity of $r \gg 1$ and $\eta \sim 1$. One finds $\eta \sim 1 - (\pi/8)^{2/5} e^{-6r/5}$, see the white dashed line in Fig. 4. This confirms the above described behaviour, which illustrates the "fragility" of a strongly squeezed state.

Finally, we repeat the same analyses for the additive-noise channel whose covariance matrix, as already mentioned above, is given by $\boldsymbol{\gamma} = \boldsymbol{\gamma}^{\mathrm{TMSV}} + \Delta \mathbb{1}_4$, where $\Delta \geq 0$ represents the noise level. Using the following parameters

$$r' = \frac{1}{2}\mathrm{arctanh}\left[\frac{\sinh(2r)}{\cosh(2r)+\Delta}\right], \quad \varphi' = \varphi\,, \quad p = \frac{1}{1+2\Delta\cosh(2r)+\Delta^2}\,, \tag{70}$$

it can also be put under the form of Eq. (9). Of course, we check that, when $\Delta \to 0$, $r' = r$, $\varphi' = \varphi$ and $p = 1$. The exact expressions of the quantum discord, the average value of the Bell operator and the non-separability threshold can be obtained using this mapping. Starting from Eq. (29), one can check that the state is separable if and only if

$$\Delta \geq 1 - e^{-2r}\,. \tag{71}$$

The expressions of the Bell violation threshold and the quantum discord can also be derived but are involved and not very enlightening. We do not reproduce them here. We only want to point out that a phenomenon similar to that observed in the pure-loss channel for large initial squeezing also happens for the additive-noise channel. Namely, as squeezing gets large, the amount of noise required to destroy the violation of the Bell inequality is reduced. All these results are summarised in Fig. 5.

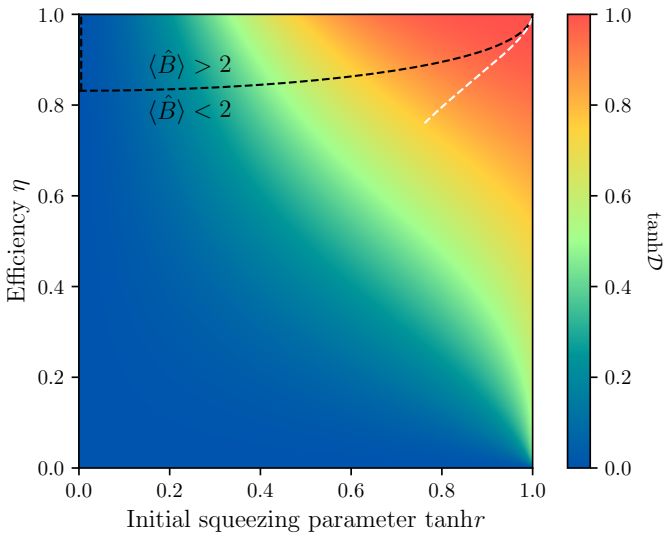

Fig. 4: Hyperbolic tangent of the quantum discord $\tanh \mathcal{D}$ computed from Eq. (15) as a function of the efficiency η and the hyperbolic tangent of the initial squeezing parameter $\tanh r$. The dashed black line represents the threshold of separability Bell inequality violation defined as the equality case in Eq. (27). The vertical piece overlaps and follow the line $r = 0$ and is represented shifted towards a non-vanishing value of r to be visible. The dashed white line shows the approximation for the threshold valid for $r \gg 1$, plotted for $r \geq 1$.

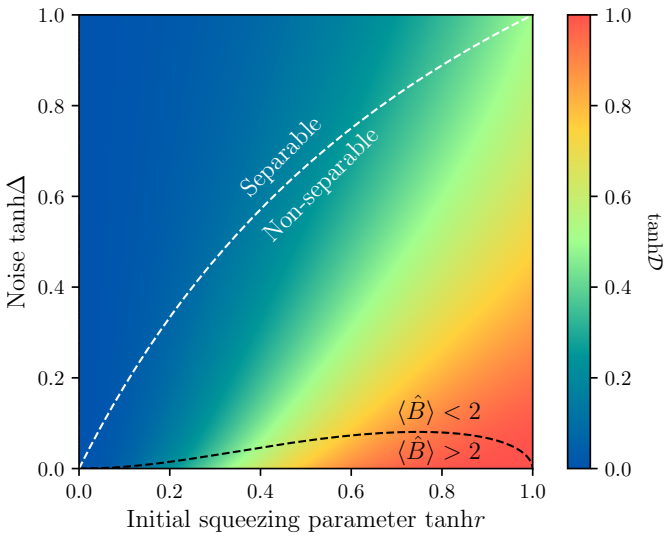

Fig. 5: Hyperbolic tangent of the quantum discord $\tanh \mathcal{D}$ computed from Eq. (15) as a function of the noise Δ and the hyperbolic tangent of the initial squeezing parameter $\tanh r$. The dashed white (respectively black) line represents the threshold of separability (respectively Bell inequality violation) defined as the equality case in Eq. (29) [respectively Eq. (27)].